Inorganic Chemistry
Communication

Inorg. Chem. **2010**, *49*, 5341–5343 **5341**
DOI: 10.1021/ic100374j

Synthesis of Bimetallic Uranium and Neptunium Complexes of a Binucleating Macrocycle and Determination of the Solid-State Structure by Magnetic Analysis

Polly L. Arnold,*,† Natalie A. Potter (née Jones),† Nicola Magnani,‡ Christos Apostolidis,‡ Jean-Christophe Griveau,‡ Eric Colineau,‡ Alfred Morgenstern,‡ Roberto Caciuffo,*,‡ and Jason B. Love*,†

†*School of Chemistry, University of Edinburgh, Edinburgh EH9 3JJ, U.K., and* ‡*European Commission, Joint Research Centre, Institute for Transuranium Elements, Postfach 2340, D-76125 Karlsruhe, Germany*

Received February 24, 2010

Syntheses of the bimetallic uranium(III) and neptunium(III) complexes $[(UI)_2(L)]$, $[(NpI)_2(L)]$, and $[\{U(BH_4)\}_2(L)]$ of the Schiff-base pyrrole macrocycles L are described. In the absence of single-crystal structural data, fitting of the variable-temperature solid-state magnetic data allows the prediction of polymeric structures for these compounds in the solid state.

The understanding of the magnetic behavior of actinide complexes, in particular multimetallic systems, lags well behind that of 3d and 4f metals. This is because the strong spin−orbit interactions, strong electron correlations, ligand-field effects, and 5f/6d occupancy in these heavy 5f metal complexes make the prediction and understanding of the interactions difficult.[1] While 4f metal cations with intrinsically high anisotropies have been used to great effect in the synthesis of single-molecule magnets (SMMs),[2] the incorporation of actinide cations offers the prospect of much stronger magnetic exchange interactions than 4f cations and large anisotropies, so such complexes are potentially rewarding targets for the synthesis of high-T_c SMMs.

The nature of the 5f states in the actinide metals has already been shown to give rise to some extraordinary magnetic phenomena in inorganic materials such as unconventional superconductivity,[3] but it is still difficult to provide a theoretical understanding of the most complex magnetic characteristics of these materials. As such, the study of simple bimetallic and oligonuclear actinide materials should provide important fundamental information. Studies of magnetic communication between two uranium centers are limited to binuclear complexes that incorporate discrete bridging ligands such as *tert*-butylimido,[4] diketimido,[5] N═C-2,2′:6′,2″-terpyridine,[6] and both *m*- and *p*-diimides, $=NC_6H_4N=$.[7] Studies on bimetallic complexes of neptunium, the first of the transuranic elements, have yet to be reported.

We have shown recently that macrocycle H_4L can only accommodate one uranyl cation in the formation of $[UO_2(THF)(H_2L)]$,[12,13] which contrasts with the wide variety of homobimetallic 3d metal complexes that can be synthesized.[14,15]

*To whom correspondence should be addressed. E-mail: polly.arnold@ed.ac.uk (P.L.A.), roberto.caciuffo@ec.europa.eu (R.C.), jason.love@ed.ac.uk; (J.B.L.). Tel: +44 131 6505429 (P.L.A. and J.B.L.). Fax: +44 131 6506453 (P.L.A. and J.B.L.).

(1) Rinehart, J. D.; Harris, T. D.; Kozimor, S. A.; Bartlett, B. M.; Long, J. R. *Inorg. Chem.* **2009**, *48*, 3382–3395.
(2) (a) Ishikawa, N.; Sugita, M.; Ishikawa, T.; Koshihara, S.-Y.; Kaizu, Y. *J. Am. Chem. Soc.* **2003**, *125*, 8694–8695. (b) Ishikawa, N. *Struct. Bonding* (*Berlin*) **2010**, *135*, 211–228. (c) Mereacre, V.; Ako, A. M.; Clerac, R.; Wernsdorfer, W.; Hewitt, I. J.; Anson, C. E.; Powell, A. K. *Chem.—Eur. J.* **2008**, *14*, 3577–3584. (d) Al Damen, M. A.; Clemente-Juan, J. M.; Coronado, E.; Marti-Gastaldo, C.; Gaita-Arino, A. *J. Am. Chem. Soc.* **2008**, *130*, 8874.
(3) (a) Santini, P.; Carretta, S.; Amoretti, G.; Caciuffo, R.; Magnani, N.; Lander, G. H. *Rev. Mod. Phys.* **2009**, *81*, 807–863. (b) Moore, K. T.; van der Laan, G. *Rev. Mod. Phys.* **2009**, *81*, 235–298.
(4) Spencer, L. P.; Schelter, E. J.; Yang, P.; Gdula, R. L.; Scott, B. L.; Thompson, J. D.; Kiplinger, J. L.; Batista, E. R.; Boncella, J. M. *Angew. Chem., Int. Ed.* **2009**, *48*, 3795–3798.
(5) Schelter, E. J.; Veauthier, J. M.; Graves, C. R.; John, K. D.; Scott, B. L.; Thompson, J. D.; Pool-Davis-Tournear, J. A.; Morris, D. E.; Kiplinger, J. L. *Chem.—Eur. J.* **2008**, *14*, 7782–7790.
(6) Schelter, E. J.; Wu, R. L.; Scott, B. L.; Thompson, J. D.; Morris, D. E.; Kiplinger, J. L. *Angew. Chem., Int. Ed.* **2008**, *47*, 2993–2996.
(7) Rosen, R. K.; Andersen, R. A.; Edelstein, N. M. *J. Am. Chem. Soc.* **1990**, *112*, 4588–4590.
(8) Avens, L. R.; Bott, S. G.; Clark, D. L.; Sattelberger, A. P.; Watkin, J. G.; Zwick, B. D. *Inorg. Chem.* **1994**, *33*, 2248–2256.
(9) (a) Karraker, D. G.; Stone, J. A.; Jones, E. R.; Edelstein, N. *J. Am. Chem. Soc.* **1970**, *92*, 4841. (b) Karraker, D. G.; Stone, J. A. *J. Am. Chem. Soc.* **1974**, *96*, 6885–6888.
(10) (a) Mishra, S. *Coord. Chem. Rev.* **2008**, *252*, 1996–2025. (b) Sharma, M.; Eisen, M. S. Metallocene organoactinide complexes. *Organometallic and Coordination Chemistry of the Actinides*; Springer-Verlag: Berlin, Germany, 2008; Vol. *127*, p 85.
(11) Den Auwer, C.; Llorens, I.; Moisy, P.; Vidaud, C.; Goudard, F.; Barbot, C.; Solari, P. L.; Funke, H. *Radiochim. Acta* **2005**, *93*, 699–703.
(12) Arnold, P. L.; Blake, A. J.; Wilson, C.; Love, J. B. *Inorg. Chem.* **2004**, *43*, 8206–8208.
(13) (a) Arnold, P. L.; Patel, D.; Wilson, C.; Love, J. B. *Nature* **2008**, *451*, 315–317. (b) Arnold, P. L.; Patel, D.; Blake, A. J.; Wilson, C.; Love, J. B. *J. Am. Chem. Soc.* **2006**, *128*, 9610–9611. (c) Berard, J. J.; Schreckenbach, G.; Arnold, P. L.; Patel, D.; Love, J. B. *Inorg. Chem.* **2008**, *47*, 11583–11592.
(14) Givaja, G.; Volpe, M.; Leeland, J. W.; Edwards, M. A.; Young, T. K.; Darby, S. B.; Reid, S. D.; Blake, A. J.; Wilson, C.; Wolowska, J.; McInnes, E. J. L.; Schroder, M.; Love, J. B. *Chem.—Eur. J.* **2007**, *13*, 3707–3723.
(15) Love, J. B. *Chem. Commun.* **2009**, 3154–3165.
(16) (a) Sessler, J. L.; Melfi, P. J.; Tomat, E.; Callaway, W.; Huggins, M. T.; Gordon, P. L.; Keogh, D. W.; Date, R. W.; Bruce, D. W.; Donnio, B. *J. Alloys Compd.* **2006**, *418*, 171–177. (b) Sessler, J. L.; Melfi, P. J.; Seidel, D.; Gorden, A. E. V.; Ford, D. K.; Palmer, P. D.; Tait, C. D. *Tetrahedron* **2004**, *60*, 11089–11097.

Published on Web 05/26/2010

Scheme 1. Synthesis of Binuclear U^{III} and Np^{III} Complexes of the Schiff-Base Pyrrolic Macrocycles H_4L, H_4L', and H_4L''

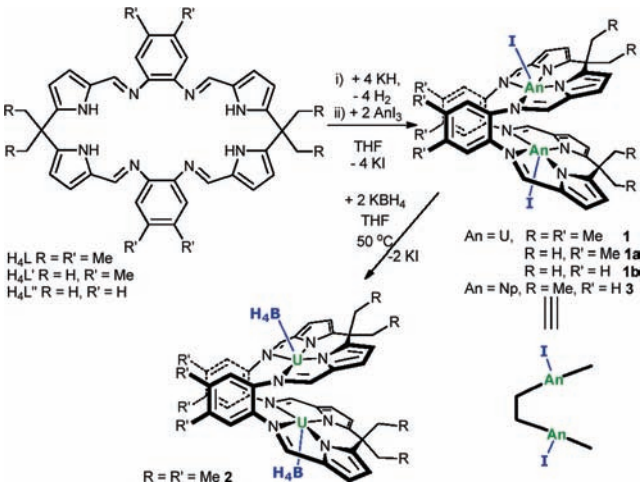

Related ligands have also been used by Sessler and co-workers to bind the neptunyl $[NpO_2]^{2+}$ cation and have been developed for colorimetric sensing applications.[16] We reasoned that binding two low-oxidation-state actinide cations in L would allow the study of the magnetic behavior of a simple binuclear system because, in the trivalent state, U^{III} is an f^3 ion and Np^{III} is an f^4 ion, so the total spin could be significant in complexes of either actinide.

The reaction between UI_3 and the potassium salt K_4L in tetrahydrofuran (THF) at −78 °C afforded a green slurry, which became red upon warming to 25 °C (Scheme 1). After workup, a dark-red, toluene-soluble powder of $[(UI)_2(L)]$ (**1**), was isolated in 90% yield.[17] We have also synthesized the permethyl analogue of **1** (R = H, R′ = Me), **1a**, and the unmethylated analogue **1b**, in which R = R′ = H. The reaction of **1** with KBH_4 in THF at 50 °C formed cleanly the binuclear uranium(borohydride) complex $[\{U(BH_4)\}_2(L)]$ (**2**) in 79% yield, which was isolated as a dark-red, toluene-soluble powder.[18] Furthermore, the addition of solid K_4L in portions to a THF slurry of $NpI_3(THF)_4$ at 25 °C afforded a dark-red-brown, toluene-soluble crystalline powder of $[(NpI)_2(L)]$ (**3**).[19] This represents a rare example of a Np^{III} coordination complex and, to our knowledge, the first bimetallic Np^{III} complex. In the lower oxidation states (III+ and IV+), the coordination and organometallic chemistry of neptunium is dominated by homoleptic halides and amides such as $NpI_3(THF)_4$ and $[Np(N\{SiMe_3\}_2)_3]$,[8] neptunocene $[Np^{IV}(\eta^8\text{-}C_8H_8)_2]$ and $K[Np^{III}(\eta^8\text{-}C_8H_8)_2]$,[9] $[Cp_3Np]$, and a handful of mixed halide amide or organometallic halide complexes such as $CpNpCl_3$[10] and adducts of heterocyclic N-donor chelators of relevance to the biological uptake of Np in place of Fe^{III}.[11]

All of the complexes have been fully characterized (see the Supporting Information, SI), and the FTIR spectrum of the borohydride region of **2** displays absorptions at 2451, 2211, and 1187 cm^{-1}, which suggests μ_3 coordination of the hydrides

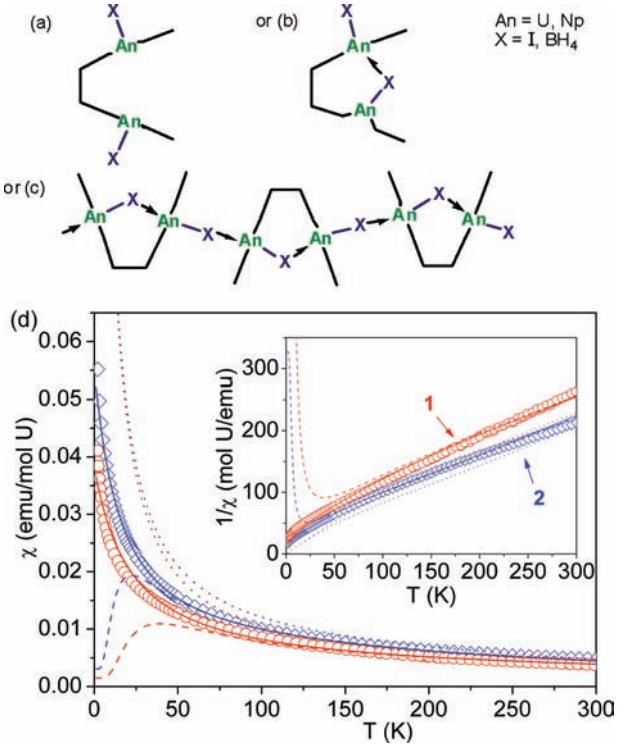

Figure 1. (a−c) Schematic structures possible for **1** and **2** (X = I, BH_4) and magnetic susceptibility data for **1** (circles) and **2** (diamonds) as a function of the temperature. $1/\chi$ vs T is plotted in the inset, and the calculated data for the structure are (a) dotted line, (b) dashed line, and (c) solid line.

to the metal, similar to that seen in $[U(BH_4)_4(THF)_2]$ and $[U(BH_4)_4]$.[20] Unfortunately, we have been unable to grow single crystals suitable for X-ray structural analysis of any of these complexes and so cannot provide definitive structural information.

The geometry of these molecules is potentially interesting because there is the possibility that the two An^{III} cations can undergo magnetic superexchange coupling through a bridging halide or borohydride.[21] Three possible structures that should exhibit distinct magnetic exchange behavior are shown schematically in Figure 1. The two mononuclear structures suggested are based on the variety of structural types shown for d-block metal complexes of L.[15] The absence of coordinating solvents and the fact that the products do not crystallize readily are indications that these materials may be polymeric in the solid state (Figure 1c).

Variable-temperature magnetic susceptibility studies were carried out on **1**−**3** in the temperature range 2−300 K in applied fields of 1 and 7 T. The results for **1** and **2**, obtained at 1 T, are shown in Figure 1. If the U^{III} ions are magnetically isolated (Figure 1a), the ligand field will dominate the magnetic behavior in the whole temperature range, defined by an effective Hamiltonian in an axial ligand field $H_{LF}' = \tilde{B}_2^0 O_2^0 + \tilde{B}_2^2 O_2^2$ with a $|J_z = \pm^1/_2, \pm^3/_2\rangle$ pseudo quartet ground state (see the SI). Although this model can qualitatively reproduce the trend displayed by magnetization measurements

(17) Data for **1**: red solid. Yield: 214 mg (90%). Anal. Calcd for $U_2I_2C_{46}H_{48}N_8$: C, 36.38; H, 2.91; N, 8.08. Found: C, 36.42; H, 2.97; N, 7.97.

(18) Data for **2**: dark-red solid. Yield: 44 mg (79%). Anal. Calcd for $U_2B_2C_{46}H_{56}N_8$: C, 45.34; H, 4.63; N, 9.19. Found: C, 45.30; H, 4.71; N, 9.03. FTIR (Nujol, cm^{-1}): 2451 (m, B−H stretch), 2211 (m, B−H stretch), 1187(w, B−H bridging deformation).

(19) Data for **3**: red-brown solid. Yield: 405 mg (98%). Anal. Calcd for $Np_2I_2C_{46}H_{48}N_8$: Np, 32.90. Found: Np, 32.5 (gravimetric), 33.22 (radiometric).

(20) (a) Banks, R. H.; Edelstein, N. M.; Rietz, R. R.; Templeton, D. H.; Zalkin, A. *J. Am. Chem. Soc.* **1978**, *100*, 1957–1958. (b) Rietz, R. R.; Edelstein, N. M.; Ruben, H. W.; Templeton, D. H.; Zalkin, A. *Inorg. Chem.* **1978**, *17*, 658–660.

(21) Rinehart, J. D.; Bartlett, B. M.; Kozimor, S. A.; Long, J. R. *Inorg. Chim. Acta* **2008**, *361*, 3534–3538.

at different fields, electron paramagnetic resonance measurements would be desirable to provide the most sensitive technique to test the wave function composition. If a $U^{III}U^{III}$ pair is present (Figure 1b), the effective Hamiltonian can be written as $H_{dim} = H_{LF}'(1) + H_{LF}'(2) + \mathcal{J}\,\mathbf{J}_1\mathbf{J}_2$ where $\mathcal{J}$ is the exchange integral, **J** is the total angular momentum operator, and the indices 1 and 2 label the two U^{III} sites. Numerical full diagonalization of H_{dim} shows that the experimental susceptibility curves cannot be reproduced within these models in the whole temperature range and antiferromagnetic exchange must be considered to reproduce the high-temperature $1/\chi$ values. The dashed lines in Figure 1 correspond to a parameter choice of $\mathcal{J} = 3.5$ K and $\tilde{B}_2^0 = 172$ K in the case of **1** and $\mathcal{J} = 2$ K and $\tilde{B}_2^0 = 82$ K in the case of **2**. However, this dimeric model does not reproduce the low-temperature behavior because the exchange splitting between the nonmagnetic singlet ground state and the excited states of the dimeric units is too large, resulting in a maximum of $\chi(T)$. A small amount of paramagnetic impurity in the sample would generate a Curie tail deviation from the humped curve, but no kink is visible in the experimental $\chi(T)$ curves. More complex magnetic associations, such as tetramers, have also been considered and found to be inconsistent with the measured susceptibility curves.

In the case of the polymeric chain structure (Figure 1c), the magnetic system cannot be constrained to a finite dimensionality and a mean-field (MF) approach is best suited to treat exchange interactions. The inverse susceptibility can then be written as $1/\chi = 1/\chi_0 - \lambda$, where χ_0 is the single-ion susceptibility and λ is determined by the antiferromagnetic exchange integrals over different sites. The solid lines in Figure 1 are the results of MF calculations, for $\tilde{B}_2^0 = 172$ K and $\lambda = 26.1$ mol of U/emu for the iodide **1** and $\tilde{B}_2^0 = 82$ K and $\lambda = 17.6$ mol of U/emu for borohydride **2**. The good agreement between experimental observations and calculated values is strong evidence that these materials are polymeric in the solid state. This conclusion is not affected by the particular choice of the ground state because the same result regarding exchange interactions would be obtained for a $|J_z = \pm{}^9/_2\rangle$ doublet ground state.

The variable-temperature data for the Np complex **3**, measured in a 1 T field between 2 and 300 K, are shown in Figure 2. The reciprocal susceptibility (shown in the inset) is essentially linear above 20 K and points toward an effective magnetic moment of 2.43 μ_B. Although this is apparently compatible with a $|J_z = \pm 4\rangle$ ground-state doublet (dashed line), a better fit of the low-temperature part is obtained by considering a different scenario, namely, a $|J_z = \pm 3\rangle$ ground-state level separated by 206 K from the first excited $|J_z = \pm 2\rangle$ level (full black line). The slight remaining discrepancy between the experiment and calculations below 5 K may be

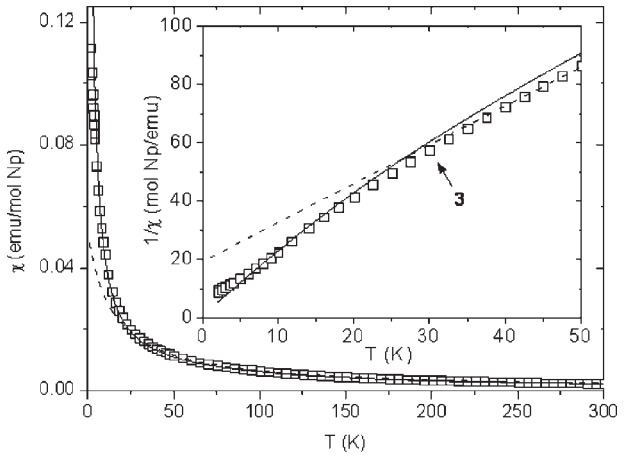

Figure 2. Magnetic susceptibility data for **3** (squares) as a function of the temperature. An expansion of the reciprocal susceptibility at low temperatures is shown in the inset. The full and dashed lines are the calculated ligand-field susceptibility for two different energy spectra of Np^{III}.

attributed to either the influence of nonaxial ligand-field terms, which can give rise to a nonmagnetic singlet or to magnetic superexchange between the 5f centers. While it is impossible to be more precise on this point with the limited available data, a comparison with the magnetic behavior of **1** and **2** allows us to infer that the superexchange coupling in **3**, be it dimeric or polymeric, is at least 1 order of magnitude smaller. This feature can be attributed to the smaller radial extension of the 5f shell with increasing f electron number.

In conclusion, the synthesis of the binuclear $[(AnX)_2(L)]$ complexes of the Schiff-base pyrrole macrocycle L (An = U, Np, X = I; An = U, X = BH_4) is straightforward, but the complexes do not crystallize, even for three different variants of the ligand. The solid-state structures are suggested by variable-temperature magnetometry to be polymeric and display relatively strong antiferromagnetic coupling between the metal centers.

Acknowledgment. We gratefully acknowledge financial support from Dr. Paul Roussel at the Atomic Weapons Establishment, the Royal Society, the EU Actinet programme and Actinet Grant 07-11, the Alexander von Humboldt Foundation, the U.K. EPSRC, and the European Commission programme Training and Mobility of Researchers. We also thank Dr. Rachel Eloirdi for helpful discussions.

Supporting Information Available: Full experimental details including some crystal growth studies, SQUID data, and analyses for **1**, **1a**, **1b**, **2**, and **3**. This material is available free of charge via the Internet at http://pubs.acs.org.